Design of a Hybrid Adaptive Filtering System for Handwriting Tremor Suppression

Opeyemi Emmanuel Agunbiade
Department of Electrical and Electronics Engineering,
School of Electrical Systems Engineering
Federal University of Technology, Akure
Ondo State, Nigeria

Brendan Ubochi
Department of Electrical and Electronics Engineering,
School of Electrical Systems Engineering,
Federal University of Technology, Akure
Ondo State, Nigeria

ABSTRACT
Parkinson's disease is a neurological condition that can affect the ability to control limb movements precisely, resulting in involuntary hand tremors that may interfere with handwriting. This study presents a convex-combination hybrid adaptive filtering system that suppresses handwriting tremor while preserving voluntary hand motion. Tri-axial accelerometer recordings drawn from the PD-BioStampRC21 dataset were converted into a scalar magnitude signal, cleaned of outliers and DC offset, normalised, and separated in frequency using a fourth-order zero-phase Butterworth band-pass filter (3-10 Hz) to obtain a tremor-reference signal within an Active Noise Control (ANC) framework. Least Mean Squares (LMS) and Recursive Least Squares (RLS) adaptive filters were implemented in parallel, and their outputs were dynamically combined using a sigmoid-bounded convex-combination supervisor. A covariance-condition guard was incorporated to limit the numerical ill-conditioning that was observed in the RLS inverse covariance matrix. Performance was evaluated using mean square error (MSE), steady-state MSE, and convergence time across 34 real accelerometer recordings. The hybrid filter achieved an overall mean MSE of 0.07420, a steady-state MSE of 0.07022, and a convergence time of 1.1118 s, compared with 0.08343, 0.07327, and 2.4206 s for standalone LMS, and 0.07425, 0.07092, and 1.1329 s for standalone RLS. These results show that the hybrid system retains the rapid tracking behaviour of RLS while approaching the steady-state stability of LMS, providing a basis for further development of tremor suppression methods.

General Terms
Signal Processing, Adaptive Filtering, Biomedical Engineering, Algorithms

Keywords
Adaptive filtering; hand tremor; hybrid filter; Least Mean Squares; Recursive Least Squares; convex combination; Parkinson's disease; Active Noise Control

1. INTRODUCTION
Parkinson's disease progressively affects the nervous system, and its impact on movement shows up through motor symptoms such as tremor, bradykinesia, rigidity, and postural impairment. Tremor, one of the most noticeable motor symptoms, can appear at rest, although its expression is also affected by posture, voluntary movement, and the individual's motor state [1]. Because involuntary rhythmic oscillation is superimposed on intended motion, it disrupts activities demanding precision and coordination (handwriting being a clear example), even minor unwanted deviations distort the accuracy and smoothness of a written trajectory [2].

Wearable inertial sensing has become an attractive way of quantifying tremor objectively outside clinical settings [3]. [4] confirmed the applicability of inertial sensors for quantitatively measuring tremor. [5] showed that consumer-grade accelerometry can yield feasible tremor measures, [6] demonstrated wearable accelerometers during drawing tasks. However, an accelerometer signal recorded during a functional task is never composed of tremor alone: it is a composite of intended movement, involuntary tremor, and sensor-related disturbance. A tremor-suppression system must therefore separate the unwanted oscillatory component from the intended movement, since excessive removal of high-frequency or time-varying content risks distorting the voluntary motion itself [7, 8]. Butterworth band filtering in the 3─9 Hz range has also proven effective at pulling pathological tremor apart from broader upper-limb motor activity [9].

Adaptive filtering suits this class of non-stationary signal-separation problem because its coefficients update continuously as new samples arrive. Among the available algorithms, Least Mean Squares (LMS) is attractive for its low computational cost and simple gradient-based update. However, its convergence speed is strongly tied to the step size and can be slow following a sudden change in the tremor pattern [7, 10]. Recursive Least Squares (RLS) converges considerably faster by exploiting second-order (covariance) information, but at higher computational cost and risk of numerical instability when the inverse covariance matrix becomes ill-conditioned [11]. [12] point out that RLS tracks concept drift in streaming data faster than LMS due to its second-order updates, but this comes at the cost of more numerical overhead and sensitivity which is why hybridizing the two is recommendable. Because the two algorithms possess complementary strengths and weaknesses, a combined structure offers a principled way of obtaining both fast tracking and stable steady-state performance rather than depending on either filter alone.

This paper presents the design, MATLAB implementation, and multi-recording evaluation of a convex-combination LMS-RLS hybrid adaptive filter for handwriting tremor suppression, embedded within an Active Noise Control (ANC) signal model. Both component filters operate concurrently on real tri-axial accelerometer recordings, and their outputs are blended using a sigmoid-bounded, error-driven mixing coefficient.

A covariance-condition guard was added to limit numerical ill-conditioning of the RLS covariance matrix. The system is evaluated using mean square error, steady-state MSE, and convergence time across 34 real PD-BioStampRC21 recordings [13], providing quantitative evidence for the practical value of combining complementary adaptive filters for this application.

2. RELATED WORKS

Several studies have investigated mechanical, wearable, and algorithmic approaches to the suppress hand tremor. [14] developed a wearable gyroscope-and-actuator device that reduced tremor by up to 92.6%, while [15] proposed a finger-tremor-suppression orthosis using an LMS-controlled PVC-gel linear actuator, achieving suppression above 65% at the fingertip. [16] [17] reported large reductions using permanent-magnet actuators combined with notch filters and fuzzy controllers (up to 97% and 88.4%, respectively). These show that active tremor-suppression hardware is feasible, but generally rely on fixed-parameter or non-adaptive control.

[7] analysed Filtered-x LMS, Filtered-x NLMS, and a hybrid Filtered-x LMS-NLMS structure for suppressing simulated hand tremor within an Active Noise Control (ANC) arrangement, achieving the fastest convergence (4000 samples) and lowest steady-state MSE (−28 dB) with the hybrid configuration, and proposing a filtered-sinusoid Fsinx-LMS variant for the non-linear dynamics of Parkinsonian tremor. This is the same ANC philosophy that involves estimating an unwanted tremor component and subtracting it from the desired signal as adopted in the present study, though the earlier study relied on synthetic tremor models rather than real accelerometer recordings.

[2] extended this to a smart-pen prototype embedding Filtered-x LMS, Filtered-x NLMS, a combined Filtered-x LMS/NLMS structure, RLS, and a Kalman filter, all implemented on a teensy 4.1 microcontroller, and evaluated using real handwriting signals from the NewHandPD dataset and a shaking table. Although RLS achieved the lowest steady-state MSE (−53 dB), the Kalman filter converged around eight times faster and was chosen for the physical prototype, so as to demonstrate that the fastest-converging algorithm is not always the lowest-error one. This trade-off directly motivates the convex-combination hybrid adopted in this study.

Convex-combination adaptive-filter architectures have also been explored outside tremor suppression. [18] reviewed convex combinations of adaptive filters, showing that a bounded mixing coefficient can blend parallel filter outputs to exploit complementary convergence behaviour; [19] demonstrated a similar structure for hearing-aid feedback cancellation; [20] [21] reported benefits from combined LMS/RLS and cascaded adaptive structures in biomedical denoising.

3. MATERIALS AND METHODS

3.1. System Overview and Dataset

This study system adopts an Active Noise Control (ANC) style signal-processing arrangement, in which the measured hand acceleration is treated as the desired signal and a frequency-selected tremor component serves as the adaptive reference input. The complete pipeline which comprises of data validation, magnitude computation, preprocessing, reference-signal construction, parallel LMS/RLS filtering, covariance guarding, convex combination, and performance evaluation was implemented entirely in MATLAB, following the structure summarised in Figure 1.

The tri-axial accelerometer recordings used for this study were obtained from the PD-BioStampRC21 dataset, a real-world wearable-sensor study of Parkinson's disease patients [13]. Right-hand recordings identified by the rh_ID naming convention were processed, with each file containing tri-axis (x, y, z) acceleration measurements. A working sampling frequency of 50 Hz and a maximum of 5,000 samples per recording (≈ 100 s) were used consistently across all experiments (as summarised in Table 1).

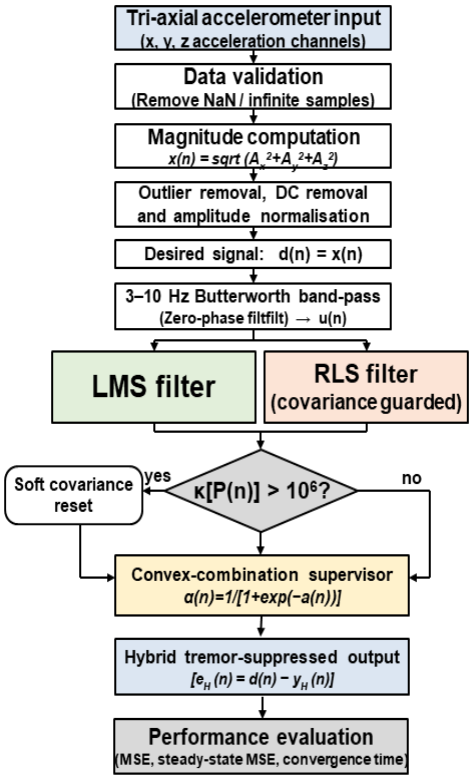


Figure 1. Workflow of the hybrid adaptive tremor-suppression system, from raw tri-axial accelerometer input to the performance-evaluation stage.

Table 1. Dataset and signal-processing parameters

Parameter	Value Used	Purpose
Working sampling frequency	50 Hz	Signal processing and time-axis calculation
Maximum samples per recording	5,000	Limits recording length processed (≈100 s)
Accelerometer axes	x, y, z	Tri-axis hand-motion measurement
Signal representation	Magnitude	Combines the three acceleration axes
Tremor reference band	3-10 Hz	Provides adaptive reference signal
DC removal	Mean subtraction	Centers the signal
Amplitude normalisation	Peak absolute value	Controls signal amplitude
Reference filter	4th-order Butterworth	Tremor-reference extraction
Zero-phase filtering	filtfilt	Avoids phase delay

3.2. Signal Preprocessing

Samples containing non-finite values (NaN or infinite entries) were first removed from the three accelerometer axes. The valid x, y, and z measurements were then combined into a scalar magnitude signal [4, 6]:

$$x(n) = \sqrt{[A_x^2(n) + A_y^2(n) + A_z^2(n)]} \quad (1)$$

Where A_x, A_y, and A_z denote the three accelerometer-axis measurements at sample n. The magnitude signal was processed using linear-interpolation outlier replacement, after which the signal mean was removed and the result normalised by its peak absolute value [7]:

$$x_n(n) = \frac{[x(n) - \bar{x}]}{max|x(n) - \bar{x}|} \quad (2)$$

where $\bar{x}$ is the mean of the magnitude signal.

The corresponding time vector was defined as $t(n) = \frac{n-1}{f_s}$ with f_s = 50 Hz, giving an analysis duration of approximately 100 s for a 5,000-sample recording.

3.3. Construction of Desired and Tremor-Reference Signals

Rather than requiring a separately recorded clean handwriting trajectory, the desired signal for the ANC arrangement was defined directly from the preprocessed magnitude signal:

$$d(n) = x_n(n) \quad (3)$$

A fourth-order Butterworth band pass filter with a 3-10 Hz passband was then applied to $x_n(n)$ using MATLAB's zero-phase filtfilt function to obtain the tremor-reference signal [7, 6]:

$$u(n) = BP_{3-10}Hz\{x_n(n)\} \quad (4)$$

[22] used the same technique to isolate the 3-7 Hz tremor band from wearable inertial data. This isolation matters for real-life monitoring, but it has to be done without distorting the person's actual voluntary arm movement. Because 'filtfilt' applies the filter in both the forward and reverse directions, the resulting reference signal has no net phase delay relative to d(n), preserving the temporal alignment required by the ANC formulation. The tremor-suppressed output is subsequently obtained from [7]:

$$e(n) = d(n) - y(n) \quad (5)$$

where y(n) is the adaptive filter's estimate of the unwanted tremor contribution.

3.4. Least Mean Squares (LMS) Filter

The LMS filter uses an eight-tap coefficient vector operating on the reference vector u(n). Its output and instantaneous error are given by [7, 23]

$$y_{LMS}(n) = w^T_{LMS}(n)\, u(n) \quad (6)$$

$$e_{LMS}(n) = d(n) - y_{LMS}(n) \quad (7)$$

where $y_{LMS}(n)$ is the estimated output generated by the filter at instant n, $w^T_{LMS}(n)$ represents the transpose of the adaptive filter coefficient vector, $u(n)$ denotes the input signal vector containing the current and delayed samples of the reference signal, $E_{LMS}(n)$ represents the instantaneous error signal between the desired signal and the estimated filter output, and $d(n)$ is the desired signal to be approximated by the adaptive filter.

A gradually decreasing step size was used to permit larger coefficient adjustments early in adaptation while progressively reducing the update magnitude thereafter: [23]

$$\mu(n) = \frac{\mu_0}{1 + \gamma n} \quad (8)$$

with μ_0 = 0.01 as the initial step size and γ = 0.0005 controlling the rate of decay. The LMS coefficient update is then [7, 10]

$$w_{LMS}(n) = w_{LMS}(n-1) + \mu(n)\, e_{LMS}(n)\, u(n) \quad (9)$$

3.5. Recursive Least Squares (RLS) Filter and Covariance Guarding

The RLS filter likewise uses an eight-tap coefficient vector, with the inverse covariance matrix initialised as [11]

$$P(0) = (1/\delta)\, I \quad (10)$$

where δ = 10 and I is the identity matrix. At each iteration, the RLS output and error are [11]

$$y_{RLS}(n) = w^T_{RLS}(n)\, u(n) \quad (11)$$

$$e_{RLS(n)} = d(n) - y_{RLS}(n) \quad (12)$$

The RLS gain vector is computed using a forgetting factor λ = 0.98: [11]

$$K(n) = \frac{P(n-1)u(n)}{[\lambda + u^T(n)P(n-1)u(n)]} \quad (13)$$

and the coefficient vector and inverse covariance matrix are updated according to [11]

$$w_{RLS}(n) = w_{RLS}(n-1) + K(n)\, e_RLS(n) \quad (14)$$

$$P(n) = (1/\lambda)[P(n-1) - K(n)u^T(n)P(n-1)] \quad (15)$$

During recursive adaptation, the covariance matrix P(n) can become ill-conditioned as signal statistics vary, a limitation well documented in the adaptive-filtering literature [11]. [24] also shows mathematically that RLS's exponential forgetting mechanism runs into matrix inversion errors and severe ill-conditioning once the process starts tracking non-stationary signals which is exactly why covariance regularization becomes necessary.

To guard against this, the condition number of P(n) was monitored at every iteration:

$$\kappa_P(n) = cond[P(n)] \quad (16)$$

A threshold of 10^6 was adopted for the numerical guard. Whenever (n) > 10^6, a soft reset was applied rather than a full replacement of P(n), blending the current covariance state with its initial well-conditioned form: [11]

$$P(n) \rightarrow (1-\rho)P(n) + \rho(1/\delta)\, I \quad (17)$$

with reset strength ρ = 0.5. This guard regulates the covariance state whenever it becomes ill-conditioned without otherwise altering the RLS coefficient-update law, and it was found to be necessary before RLS could be reliably incorporated as a component of the hybrid filter.

3.6. Convex-Combination Hybrid Model

Rather than permanently selecting one of the two filters, the hybrid architecture runs LMS and RLS in parallel and combines their outputs using a time-varying mixing coefficient α(n), obtained from an unconstrained internal state a(n) through a sigmoid transformation: [18, 19]

$$\alpha(n) = \frac{1}{1 + exp(-a(n))} \quad (18)$$

which constrains 0 < α(n) < 1. The hybrid output and hybrid error are then [18, 19]

$$y_H(n) = \alpha(n)\, y_{RLS}(n) + [1 - \alpha(n)]\, y_{LMS}(n) \quad (19)$$

$$e_H(n) = d(n) - y_H(n) \quad (20)$$

When α(n) approaches 1, the hybrid relies more heavily on the fast-tracking RLS output; when it approaches 0, the more stable LMS output dominates. Because α(n) varies continuously between these limits, the hybrid output transitions smoothly rather than switching abruptly between the two parent filters.

3.7. Supervisor Update and Normalisation

The internal mixing state a(n) is updated using the hybrid error and the difference between the two parent-filter outputs. The instantaneous gradient term is [18, 19]

$$g(n) = e_H(n)[y_{RLS}(n) - y_{LMS}(n)]\,\alpha(n)[1 - \alpha(n)] \quad (21)$$

A smoothed gradient-power estimate reduces sensitivity to rapid fluctuations in g(n):

$$p(n) = \beta\, p(n-1) + (1-\beta)\, g^2(n) \quad (22)$$

and the internal mixing state is updated using power-normalised gradient adaptation: [18, 19]

$$a(n+1) = \frac{(1-\lambda_l)\, a(n) + \mu_\alpha\, g(n)}{\sqrt{p(n)} + \varepsilon} \quad (23)$$

Where μ_α is the supervisor adaptation rate, λ_l is a leakage factor, β controls gradient-power smoothing, and ε prevents division by a near-zero quantity. The internal state was constrained to $-4 \le a(n) \le 4$ before applying the sigmoid transformation. The parameter values used were μ_α = 0.5, λ_l = 0.001, β = 0.9, and ε = 10^{-4}, summarised together with the remaining filter parameters in Table 2.

[25] noted in their survey that most modern adaptive algorithms handle non-stationary environments by leaning on dynamic parameter scaling and gradient-power normalization to keep tracking performance stable.

Table 2. Adaptive filter and convex-combination parameters

Parameter	Symbol	Value	Role
Filter order (taps)	M	8	Number of adaptive coefficients
Initial LMS step size	μ_0	0.01	Initial LMS adaptation rate
LMS decay parameter	γ	0.0005	Controls step-size reduction
RLS forgetting factor	λ	0.98	Controls memory of previous samples
Initial covariance scaling	δ	10	Determines initial P(0)
RLS condition threshold	K_{th}	10^6	Triggers covariance guard
Covariance reset strength	ρ	0.5	Blends P(n) toward initial state
Mixing coefficient range	α(n)	0–1	Controls LMS/RLS contribution
Internal mixing-state range	a(n)	[−4, 4]	State used to generate α(n)
Supervisor adaptation rate	μ_α	0.5	Controls mixing-state adaptation
Normalisation constant	ε	10^{-4}	Prevents division by zero

3.8. Experimental Design and Performance Measures

The evaluation proceeded in three progressive stages. First, standalone LMS and RLS filters were compared on an initial set of recordings (rh_ID005, rh_ID015, rh_ID025) to establish baseline behaviour and expose the RLS numerical-stability problem. Second, following the introduction of the ANC signal formulation, time- and frequency-domain integrity verification, and the covariance guard, the LMS-RLS baseline comparison and the first hybrid evaluation were repeated on rh_ID015, rh_ID025, and rh_ID035. Third, four additional recordings (rh_ID005, rh_ID010, rh_ID020, rh_ID030) were processed using the same fixed methodology to check the consistency of hybrid behaviour, and the analysis was finally extended to a 34-recording macro-analysis.

Three performance measures used include mean square error (MSE), which measures the average squared difference between the desired and filtered signals; steady-state MSE, which isolates the residual error after the initial transient adaptation period; and convergence (recovery) time, defined as the time required for the error to fall below and remain within an acceptable threshold following a significant tremor-related disturbance. Together, these measures assess both the overall quality of tremor suppression and the responsiveness of each filter to changing signal conditions.

4. RESULTS AND DISCUSSION

4.1. Initial LMS versus RLS Comparison

The first evaluation compared standalone LMS and RLS on three recordings (rh_ID005, rh_ID015, rh_ID025) as summarised in Table 3. LMS produced a lower mean and steady-state MSE than RLS in all the three cases, contrary to the theoretical expectation that RLS should achieve superior steady-state accuracy. This discrepancy was traced to numerical ill-conditioning of the RLS inverse covariance matrix rather than to any inherent weakness of the algorithm itself, motivating the covariance-conditioning investigation described next.

Table 3. Initial LMS versus RLS results for three recordings

Metric	rh_ID005	rh_ID015	rh_ID025
LMS mean MSE	0.0600	0.0160	0.0597
RLS mean MSE	0.0705	0.0187	0.0689
LMS steady-state MSE	0.0788	0.0028	0.1674
RLS steady-state MSE	0.0918	0.0029	0.1751
LMS recovery time (s)	0.26	0.02	0.02
RLS recovery time (s)	0.52	0.02	0.02

4.2. RLS Numerical Stability

The condition number of the RLS covariance matrix was tracked throughout each recording. In all three initial recordings, the condition number rose from an initially well-conditioned value of approximately 2-3 to beyond 10^6 within roughly the first 20 seconds, with rh_ID015 exceeding 10^7 (the worst case observed). Figure 2 illustrates this rapid growth for rh_ID015, confirming that the RLS implementation required a numerical safeguard before it could serve as a reliable component of the hybrid system.

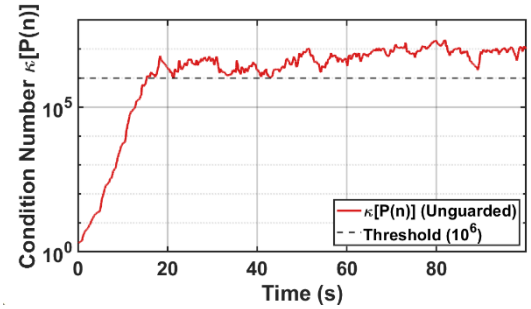


Figure 2. RLS covariance-matrix condition number (log scale) for recording rh_ID015 before covariance-condition guarding, showing rapid growth beyond the 10^6 warning threshold within approximately 20 seconds.

After incorporating the soft covariance-reset guard described by Equations 16 and 17, the condition number was held close to the 10^6 threshold for the remainder of each recording rather than continuing to diverge, as shown in Figure 3. This behaviour is consistent with the general RLS limitation reported by [11], whereby recursive covariance updates can become unstable when the underlying signal statistics change, and it supports the motivation for combined adaptive structures discussed by [21].

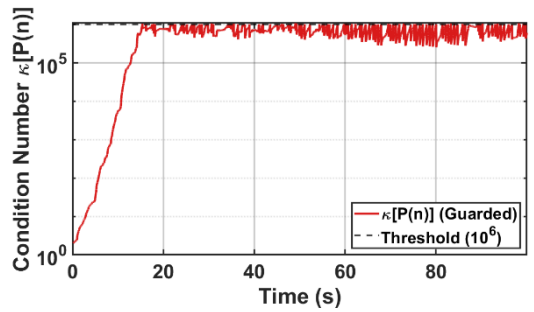


Figure 3. RLS covariance-matrix condition number for recording rh_ID015 after covariance-condition guarding, showing the condition number regulated near the 10^6 threshold instead of continuing to diverge.

4.3. ANC Signal Integrity Verification

Before proceeding to the final baseline and hybrid comparisons, the ANC signal relationship d(n) = e(n) + y(n) was verified in both the time and frequency domains. Figure 4 shows the desired signal, the adaptive estimate, and the reconstructed signal overlaid in the time domain; the close overlap confirms that the estimated tremor component and the residual (tremor-suppressed) component together reproduce the original measured signal. Figure 5 provides an independent frequency-domain check using the Fast Fourier Transform, showing that the spectral content of the retained and removed components recombines to recreate the input spectrum. These two checks strengthen confidence in the ANC formulation prior to the final hybrid comparison.

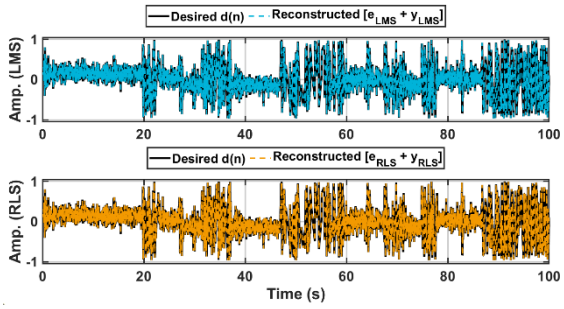


Figure 4. Time-domain verification of ANC signal integrity: desired signal, adaptive tremor estimate, and reconstructed signal.

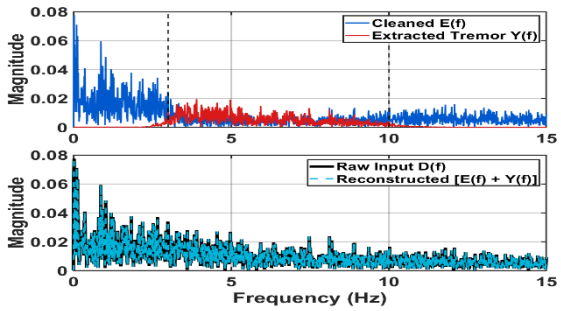


Figure 5. Frequency-domain (FFT) verification of signal integrity after tremor-band separation.

4.4. Final LMS-RLS Baseline Comparison

Following the introduction of covariance guarding, the LMS-RLS baseline comparison was repeated on rh_ID015, rh_ID025, and rh_ID035. Table 4 summarises the highlighted comparison: RLS achieved a slightly lower mean MSE (0.0958) than LMS (0.1007), while LMS exhibited marginally tighter steady-state behaviour. The most striking difference was in responsiveness as RLS recovered from a tremor-onset event in approximately 0.02 s, compared with approximately 7.0 s for LMS in the same recording.

This trade-off is relevant to handwriting, where tremor characteristics can change within a stroke. Fast recovery is useful, but speed alone is insufficient if the resulting estimate is noisy or unstable. The hybrid therefore seeks to retain RLS responsiveness while allowing LMS to contribute during steadier intervals. The objective is not to make one parent filter dominant at all times, but to use their complementary responses as signal conditions change.

Table 4. Final LMS versus RLS baseline observations (highlighted comparison)

Measure	LMS	RLS	Main Observation
Mean MSE	0.1007	0.0958	RLS slightly lower
Steady-state behaviour	Marginally tighter	More affected by noise	LMS more stable
Tremor-onset recovery	≈ 7.0 s	≈ 0.02 s	RLS much faster

4.5. Hybrid Convex-Combination Results

The hybrid stage exploits the complementary behaviour identified above. Figure 6 shows the mixing-coefficient trace α(n) for recording rh_ID035: α(n) rises toward RLS-dominant

behaviour ($\alpha \rightarrow 1$) around sudden tremor transients and falls into the 0.25-0.4 range during steadier portions of the recording so that LMS can control the residual error. This pattern differed across recordings: for rh_ID015, α(n) remained close to 1 for most of the recording, reflecting strong reliance on RLS, whereas for the more erratic rh_ID025, α(n) swung repeatedly between values near 1.0 and near 0.0, reflecting continual switching between fast RLS tracking and LMS smoothing. This behaviour confirms that the supervisor is responding to the signal itself rather than applying a single fixed weighting across all recordings.

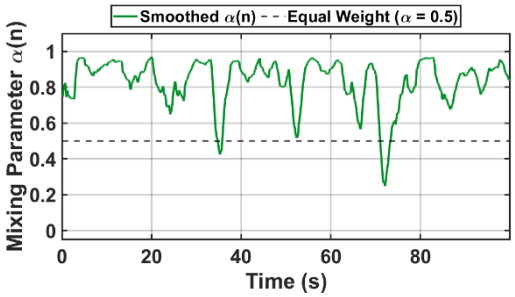


Figure 6. Hybrid mixing-parameter α(n) behaviour for recording rh_ID035, showing RLS-dominant weighting near sudden tremor transients and increased LMS contribution during steadier intervals.

Figure 7 shows the corresponding smoothed MSE traces for LMS, RLS, and the hybrid filter on rh_ID035. During large error spikes, the hybrid trace (green) declines to follow the slower LMS trace (blue); instead, the supervisor raises the RLS contribution so that the hybrid inherits RLS's rapid recovery. During quieter intervals, the situation reverses, and the hybrid trace moves toward the lower and less noisy LMS error level rather than the RLS steady-state trace (red). The hybrid is therefore not attempting to make either parent filter dominate uniformly; it continuously seeks the locally lower-error behaviour available from the two parent filters as the signal evolves. Table 5 summarises the mixing behaviour observed for the three key recordings.

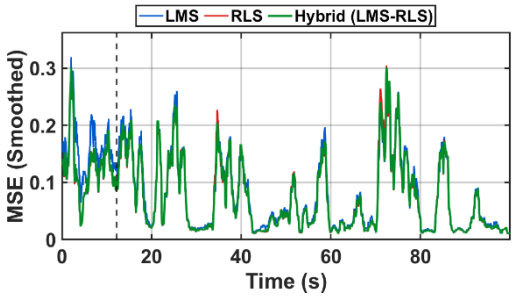


Figure 7. Hybrid Mean Square Error convergence for recording rh_ID035, comparing LMS (blue), RLS (red), and the convex-combination hybrid output (green).

Table 5. Key hybrid mixing observations for rh_ID015 rh_ID025, and rh_ID035

Recording	Mixing Behaviour	Observed Hybrid Effect
rh_ID015	α mostly near 1, small dips	Strong RLS contribution; rapid tracking
rh_ID025	α changes aggressively	Switches contribution under irregular tremor
rh_ID035	α reduces during stable regions	More LMS contribution for stability

For rh_ID025, the hybrid reduced the steady-state MSE from 0.0664 (RLS alone) to 0.0653; for rh_ID035, the hybrid matched the lowest mean error among the standalone filters (≈ 0.0783) without inheriting LMS's much longer ≈ 4.16 s recovery delay. These examples illustrate the practical value of the convex combination: the aim is a balanced operating point rather than a simple replacement of one filter by another.

4.6. Additional Dataset Validation

To reduce the risk that the observed hybrid advantage was specific to the three originally selected recordings, four additional recordings (rh_ID005, rh_ID010, rh_ID020, rh_ID030) were processed using the identical, already-fixed methodology. Figure 8 shows the mixing-parameter trace and Figure 9 the corresponding MSE convergence plot for rh_ID030, representative of the additional set. As before, the mixing coefficient varied from recording to recording, reflecting the different tremor and voluntary-motion characteristics of each subject, while the hybrid MSE trace continued to track the locally lower-error behaviour of the two parent filters. This consistency across an independent set of recordings that were not used to define the hybrid structure provides supporting evidence that the observed behaviour generalises beyond the initial three examples.

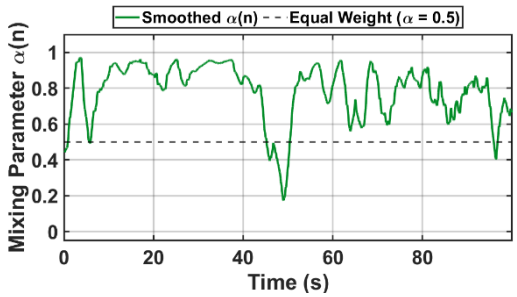


Figure 8. Hybrid mixing-parameter α(n) behaviour for an additional validation recording (rh_ID030).

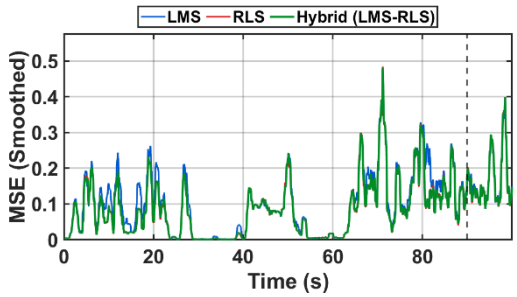


Figure 9. Hybrid Mean Square Error convergence for an additional validation recording (rh_ID030), comparing LMS, RLS, and the hybrid output.

4.7. Grand Analysis Across 34 Datasets

The most comprehensive evaluation was a macro-analysis across all 34 available recordings, summarised in Table 6. The hybrid filter achieved the lowest overall mean MSE (0.07420) among the three approaches, although the margin relative to RLS (0.07425) was small. More decisively, the hybrid also

achieved the lowest steady-state MSE (0.07022) and the fastest average convergence time (1.1118 s), compared with 1.1329 s for RLS and 2.4206 s for LMS. This combination of lowest mean MSE, lowest steady-state MSE, and fastest convergence results simultaneously is the strongest evidence in support of the convex-combination architecture, since the hybrid did not sacrifice the rapid response inherited from RLS in order to achieve improved steady-state error.

Table 6: Grand analysis across 34 datasets: LMS, RLS, and hybrid convex combination

Evaluation Metric	LMS	RLS	Hybrid Convex Combination
Overall mean MSE	0.08343	0.07425	0.07420
Steady-state MSE	0.07327	0.07092	0.07022
Convergence time (s)	2.4206	1.1329	1.1118

4.8. Discussion

The results confirm the design hypothesis underlying this study. LMS behaves in a controlled manner but responds slowly to strong tremor events; RLS responds considerably faster but is vulnerable to covariance ill-conditioning, as directly demonstrated in Section IV-B. Covariance guarding addressed the numerical dimension of this problem, but a guarded RLS filter alone would still represent only a single, fixed point in the speed-stability tradeoff space. The convex-combination supervisor adds a further layer of adaptability: when RLS is more informative, $\alpha(n)$ increases; when LMS is more informative, $\alpha(n)$ decreases. The additional four-recording validation and the 34-dataset macro-analysis both indicate that this behaviour is not restricted to the original three recordings used during development.

The results also emphasize the importance of careful signal preparation. If the desired and reference signals were poorly time-aligned, or if the tremor-reference band contained excessive unrelated content, the adaptive filters could learn an incorrect relationship between the two signals. The time- and frequency-domain integrity verification (Section IV-C) is therefore an essential part of the methodology rather than a supplementary illustration, and the use of zero-phase filtfilt filtering ensured that frequency separation did not itself introduce a relative phase delay between the signals supplied to the ANC system.

These findings should be interpreted within the scope of a MATLAB simulation study rather than a clinical trial. The desired signal used for evaluation was constructed from the raw accelerometer recording itself rather than an independently recorded clean handwriting trajectory, so the reported MSE measures the quality of this signal-separation model specifically. Future work involving an actual handwriting-trajectory reference, a wider range of tremor severities and medication states, and an embedded hardware implementation would provide a further, complementary level of validation.

4.9. Limitations of the study

The study is a MATLAB simulation and is not a clinical trial or a hardware validation. The desired signal is constructed from the accelerometer recording itself, and the reported MSE therefore evaluates the implemented signal-separation model rather than a separately measured clean handwriting trajectory. The study also notes that the PD-BioStampRC21 recordings provide valuable real-world variability but should not be assumed to represent every Parkinson's patient. Further validation with larger and more diverse clinical datasets, actual handwriting trajectories, and embedded hardware would provide additional evidence beyond the present simulation study.

5. CONCLUSION

This study presented the design, implementation, and multi-recording evaluation of a convex-combination LMS-RLS hybrid adaptive filtering system for handwriting-tremor suppression, implemented within an Active Noise Control signal model and evaluated on real PD-BioStampRC21 accelerometer recordings. Standalone LMS and RLS filters were first compared to establish their complementary characteristics, revealing both the expected LMS-RLS speed-stability tradeoff and an unexpected RLS covariance ill-conditioning problem that was subsequently addressed with a covariance-condition guard. The final convex-combination hybrid, governed by a sigmoid-bounded, error-driven mixing coefficient, allowed both filters to contribute simultaneously according to local signal behaviour. Across a 34-recording macro-analysis, the hybrid achieved the lowest overall mean MSE (0.07420), the lowest steady-state MSE (0.07022), and the fastest convergence time (1.1118 s) among the three evaluated approaches – compared with 0.08343, 0.07327, and 2.4206 s for standalone LMS, and 0.07425, 0.07092, and 1.1329 s for standalone RLS. These results demonstrate that combining complementary adaptive algorithms through a bounded convex combination can yield a more balanced response than relying on either filter individually for non-stationary handwriting-tremor signals, providing a signal-processing foundation upon which future embedded, real-time, and clinically validated tremor-suppression devices can be built.

6. REFERENCES

[1] Abusrair, A. H., Elsekaily, W., and Bohlega, S. 2022. Tremor in Parkinson's disease: From pathophysiology to advanced therapies. Tremor and Other Hyperkinetic Movements, 12, 25. https://doi.org/10.5334/tohm.712

[2] Tironi, J. C., Fernandes, A., Borges, R. C., Silva, L. A., and Parreira, W. D. 2025. A smart pen prototype with adaptive algorithms for stabilizing handwriting tremor signals in Parkinson's disease. Scientific Reports, 15, 28659. https://doi.org/10.1038/s41598-025-14196-5

[3] Lora-Millan, J. S., Delgado-Oleas, G., Benito-Leon, J., and Rocon, E. 2021. A review on wearable technologies for tremor suppression. Frontiers in Neurology, 12, 700600. https://doi.org/10.3389/fneur.2021.700600

[4] McGurrin, P., McNames, J., Wu, T., Hallett, M., and Haubenberger, D. 2020. Quantifying tremor in essential tremor using inertial sensors: Validation of an algorithm. IEEE Journal of Translational Engineering in Health and Medicine, 9, 2700110. https://doi.org/10.1109/JTEHM.2020.3032924

[5] van Brummelen, E. M. J., Ziagkos, D., de Boon, W. M. I., Hart, E. P., Doll, R. J., Huttunen, T., Kolehmainen, P., and Groeneveld, G. J. 2020. Quantification of tremor using consumer product accelerometry is feasible in patients with essential tremor and Parkinson's disease: A comparative study. Journal of Clinical Movement Disorders, 7, 4. https://doi.org/10.1186/s40734-020-00086-7

[6] Ali, S. M., Arjunan, S. P., Peters, J., Perju-Dumbrava, L., Ding, C., Eller, M., Raghav, S., Kempster, P., Motin, M.

A., Radcliffe, P. J., and Kumar, D. K. 2022. Wearable sensors during drawing tasks to measure the severity of essential tremor. Scientific Reports, 12, 5242. https://doi.org/10.1038/s41598-022-08922-6

[7] Araujo, R. S. A., Tironi, J. C., Parreira, W. D., Borges, R. C., De Paz Santana, J. F., and Leithardt, V. R. Q. 2023. Analysis of adaptive algorithms based on least mean square applied to hand tremor suppression control. Applied Sciences, 13(5), 3199. https://doi.org/10.3390/app13053199

[8] San-Segundo, R., Montero, R., Moreno-Pimentel, J., Pardo, J. M., and Gallardo-Antolin, A. 2020. Parkinson's disease tremor detection in the wild using wearable accelerometers. Sensors, 20(20), 5817. https://doi.org/10.3390/s20205817

[9] Gutowski, T., Stodulska, O., Ćwiklińska, A., Gutowska, K., Kopeć, K., Betka, M., Antkiewicz, R., Koziorowski, D., and Szlufik, S. 2025. Machine learning-based assessment of Parkinson's disease symptoms using wearable and smartphone sensors. Sensors, 25(16), 4924. https://doi.org/10.3390/s25164924

[10] Jain, D., and Beniwal, P. 2022. A novel LMS algorithm applied to adaptive noise cancellation with varying parameters. International Journal for Research in Applied Science and Engineering Technology, 10(2), 47-51. https://doi.org/10.22214/ijraset.2022.40179

[11] Shuhua, L., and Zhi, Q. 2019. An improved strong tracking variable forgetting factor RLS algorithm with low complexity for dynamic system identification. In 2019 IEEE 2nd International Conference on Electronics and Communication Engineering (ICECE) 444–450. https://doi.org/10.1109/ICECE48499.2019.9058504

[12] Igual, J., Gomes, H. M., Pfahringer, B., and Bifet, A. 2025. Linear adaptive filtering for regression in data streams. International Journal of Data Science and Analytics, 20(5), 5017–5032. https://doi.org/10.1007/s41060-025-00766-3

[13] Adams, J. L., Dinesh, K., Snyder, C. W., Xiong, M., Tarolli, C. G., Sharma, S., Dorsey, E. R., and Sharma, G. 2021. A real-world study of wearable sensors in Parkinson's disease. npj Parkinson's Disease, 7(1), 106. https://doi.org/10.1038/s41531-021-00248-w

[14] Van, H. P., and Ngo, H. Q. T. 2021. Developing an assisting device to reduce the vibration on the hands of elders. Applied Sciences, 11(23), 11115. https://doi.org/10.3390/app11115026

[15] Liu, C., and Zhang, K. 2024. A wearable finger tremor-suppression orthosis using the PVC gel linear actuator. IEEE Robotics and Automation Letters, 9, 3854–3861. https://doi.org/10.1109/LRA.2024.3369492

[16] Zamanian, A. H., and Richer, E. 2019. Adaptive notch filter for pathological tremor suppression using permanent magnet linear motor. Mechatronics, 63, 102273. https://doi.org/10.1016/j.mechatronics.2019.102273

[17] Jamaludin, H. B., As'Arry, A., Musab, R., Rezali, K. A. M., Ahmad, R. M. K. B. R., and Zarhamdy, M. B. M. 2021. Active tremor control in human-like hand tremor using fuzzy logic. Indonesian Journal of Electrical Engineering and Computer Science, 24, 108–115. https://doi.org/10.11591/ijeecs.v24.i1.pp108-115

[18] Vázquez, Á. A., Avalos, J. G., Sánchez, G., Sánchez, J. C., and Pérez, H. 2023. A comparative survey of convex combination of adaptive filters. IETE Journal of Research, 69(2), 940–950. https://doi.org/10.1080/03772063.2020.1844075

[19] Vanamadi, R., and Kar, A. 2021. Feedback cancellation in digital hearing aids using convex combination of proportionate adaptive algorithms. Applied Acoustics, 182, 108175. https://doi.org/10.1016/j.apacoust.2021.108175

[20] Kahankova, R., Martinek, R., Nedoma, J., Fajkus, M., Brablik, P., Nazeran, H., and Barnova, M. 2022. Optimization of adaptive filter control parameters for non-invasive fetal electrocardiogram extraction. PLOS ONE. 17(4) e0266807. https://doi.org/10.1371/journal.pone.0266807

[21] Pauline, S. H., Dhanalakshmi, S., and Kumar, R. 2022. Variable-stage cascaded adaptive filter technique for signal de-noising application. Circuits, Systems, and Signal Processing, 41(4), 1972–2006. https://doi.org/10.1007/s00034-021-01868-6

[22] Timmermans, N. A., Terranova, R., Soriano, D. C., Cagnan, H., Raykov, Y. P., Bucur, I. G., Bloem, B. R., Helmich, R. C., and Evers, L. J. W. 2025. A generalizable and open-source algorithm for real-life monitoring of tremor in Parkinson's disease. npj Parkinson's Disease, 11, 205. https://doi.org/10.1038/s41531-025-01056-2

[23] Li, B., Lu, B., Kou, X., Shi, Y., Yu, L., Guo, H., Lv, B., and Zeng, K. 2023. Research on variable-step-size adaptive filter algorithm with a momentum term. Applied Sciences, 13, 12077. https://doi.org/10.3390/app132112077

[24] Stotsky, A. 2025. Recursive least squares estimation with rank two updates. Automatika, 66(4), 619–624. https://doi.org/10.1080/00051144.2025.2517431

[25] Zhang, Y., Zhang, W., Zhang, L., Li, H., and Mo, W. 2026. Adaptive online convex optimization: A survey of algorithms, theory, and modern applications. Applied Sciences, 16(4), 1739. https://doi.org/10.3390/app16041739